Autonomous Control System for Precise Orbit Maintenance

Manop Aorpimai, Yoshi Hashida and Phil Palmer

Surrey Space Centre,
University of Surrey
Guildford, UK. GU2 5XH
Tel: +44 1483 259278
Fax: +44 1483 259503.
Email: M.Aorpimai@ee.surrey.ac.uk

ABSTRACT

In this paper, we describe a closed-loop autonomous control system that enables orbit operations to be performed without the need of any ground segment. The growing availability of GPS receivers on satellites provides an excellent means for autonomous orbit determination and our work builds upon previous work on orbit determination algorithms developed here at Surrey. The orbit is described using a set of epicycle parameters which provide an analytic model of LEO orbits. The parameters in this model are estimated onboard the satellite using a Kalman filter. We describe an enhancement to this software which provides both control as well as estimation of the orbit parameters and a discussion of how atmospheric drag has been included in the model. The goal of the control part of the software is to ensure that the orbital altitude of the satellite never falls outside of a prescribed window due to drag. We present results of the orbit maintenance software which has been successfully running on Surrey's mini-satellite UoSat-12. This satellite is in a 650 km altitude orbit at inclination 64.57°. The satellite has been manoeuvred into a repeat ground track orbit so that the satellite repeats its ground track every 7 days. The orbit maintenance software then attempts to maintain the satellite in its resonant orbit, and also to slowly manoeuvre the satellite into a frozen orbit so that the altitude at each pass does not vary.

1. INTRODUCTION

There is currently great interest in formation flying of small satellites in low Earth orbit to provide better remote sensing information and perform space and time variation experiments in the geospace. To achieve the missions goal, it requires tightly control [1,2] of spacecraft's position with respect to either other satellites in the formation system, the ground or inertial target in space. In some advanced single satellite missions may also require such stringent control accuracy. *TOPEX/Poseidon* mission, for example, requires that the radial position of the spacecraft be determined with an accuracy better than *13 cm* RMS in order to provide the means to determine the ocean's dynamic topography with an unprecedented accuracy. The satellite groundtrack is controlled to fly over two verification sites with the accuracy of ± 1 *km* around the reference equator crossing [3].

To maintain satellites in such stringent requirements needs the ability to maintain the orbits of satellites in LEO encountering differential effects of the Earth's oblateness and atmospheric drag. The variability of atmospheric drag, especially during periods of high solar activity, such as over the next few years, make it difficult for ground-based control to be effective, or may be not possible for some cases. Performing frequent orbit corrections from such traditional operation scheme also demands overwhelm resources from the ground segment for manoeuver planning and commanding, especially when dealing with multiple satellites. Hence, the orbit operational cost becomes dominant comparing to the overall mission budget. Attempts, therefore, have been put on improving orbit operational concept. Automation of both orbit determination and control system has become

attractive solutions, especially for small low-cost satellites [4,5].

At Surrey Space Centre (SSC), we have conduct an autonomous orbit control experiment on UoSat-12 [6] which is our first mission who posses propulsion system. The 300 kg spacecraft (see *figure 1.1*) was launched into an inclined 64.57° with an altitude of approximately 650 km. The main propose is to demonstrate number of new advanced miniature technologies, such as high solution multi-spectrum Earth imaging and low-cost propulsion system. In the spacecraft control part, it carries the developed in-house GPS receiver for supply raw GPS data to the autonomous orbit determination system. 10 cold-gas and one resistojet thrusters are used for attitude and orbit manoeuvre experiments.

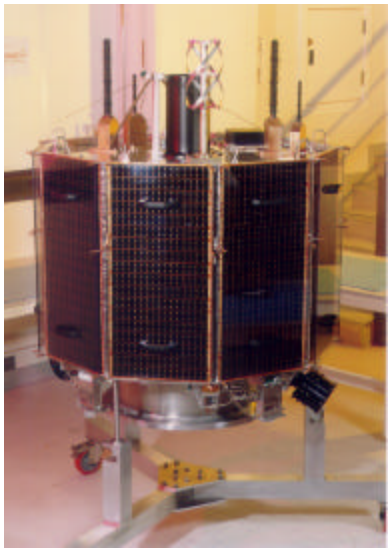

Figure 1.1 Surrey Space Centre UoSat-12

In this paper we describe the autonomous orbit maintenance system that has been flown on UoSat-12. In the next section, we shall describe the orbital dynamics modelling we have developed here at SSC. The satellite motion is described through a set of parameters which we call epicycle parameters. In section 3, we then explain the orbit determination technique which allows these parameters as well as orbital decay rate can be determined real-time onboard the spacecraft. The orbit control experiment on UoSat-12 is explained in section 4, and the orbit maintenance algorithm for keeping the satellite in a resonant orbit is described in section 5. We discuss our system integration in section 6. In section 7, we show the experimental results obtained from the spacecraft, and, finally, we draw our conclusion in the last section.

2. EPICYCLIC MOTION

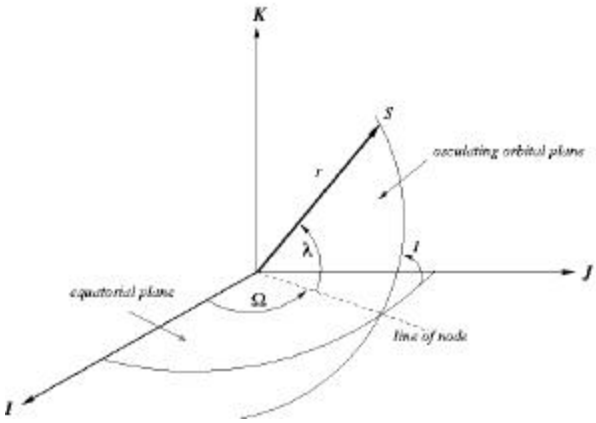

Figure 2.1 Coordinate System

2.1 Perturbed Epicycle

The epicycle description of orbit is useful to formulate the perturbed motion of near circular orbit, because its formulation is simple and has no eccentricity divisor [7].

We begin by introducing the Keplerian equations of motion in 2D which are given by:

$$\left.\begin{aligned} \ddot{r} - r\dot{l}^2 &= -\frac{1}{r^2} \\ \frac{d}{dt}\left(r^2\dot{l}\right) &= 0 \end{aligned}\right\} \qquad (2.1)$$

in some polar coordinates (r, l) , and where m is the gravitational parameter. For circular orbits, we can find a solution to *equations (2.1)* in which $r = a$ and $\dot{l} = n$ where both a and n are constants which satisfy $a^3 n^2 = m$.

Let's seek the motions of satellites in a near circular orbit ,which can be found by perturbing the trivial solution mentioned above. Let $r = a + s$ and $\dot{l} = n + e$, and ignoring second order terms in these small corrections, we can linearise and solve the *equation (2.1)* to obtain:

$$\left.\begin{aligned} s &= 2\delta a - A\cos(\alpha - \alpha_P) \\ e &= l_0 - 3\delta a + \frac{2A}{a}\sin(\alpha - \alpha_P) \end{aligned}\right\} \qquad (2.2)$$

where δ, α_P, A and l_0 are all integration constants. The angle α is defined by $\alpha = nt$. We can also show the first order correction to the orbital energy is related to $\delta$by:

$$E = -\frac{\mu}{2a}(1 - 2\delta) \qquad (2.3)$$

If we fix the *mean* orbital radius (or *semi-major axis*) as the radius of a circular orbit of the same orbital energy, then $\delta = 0$. And if we start to count the (dimensionless) time α at which satellite crosses its ascending node, then l can be identified as the *argument of latitude*. Note that $l = 0$ when $\alpha = 0$. These conditions determine two integration constants and gives:

$$\left.\begin{aligned} r &= a - A\cos(\alpha - \alpha_P) \\ l &= \alpha + \frac{2A}{a}[\sin(\alpha - \alpha_P) + \sin\alpha_P] \end{aligned}\right\} \qquad (2.4)$$

These equations then describe epicycle motion, and we call *A*, *epicycle amplitude* and α, *epicycle phase*.

Now we expand the Keplerian epicycle description of orbit to the orbit perturbed by the axisymmetric potential. We use 4 redundant coordiantes $(r \quad I \quad \Omega \quad l)$ to describe the perturbed orbit in 3D (see *figure (2.1)*), where *I* is an inclination angle and $\Omega$is an ascending node.

Because the orbital energy $E = v^2/2 + \Phi$ is still conserved under the axisymmetric gravitational field, we can defined our *mean semi-major axis a* to satisfy:

$$a = -\frac{\mu}{2E} \qquad (2.5)$$

Then the *epicycle frequency n* is obtained through $a^3 n^2 = \mu$ and remember the epicycle phase is defined by $\alpha = nt$. Under these definitions, we have shown the perturbed motion of a satellite is described by the following epicycle expression [7].

$$\left.\begin{aligned} r &= a(1+\rho) - A\cos(\alpha - \alpha_P) + ac\sin((1+k)\alpha) + \Delta_r \\ I &= I_0 + \Delta_I \\ \Omega &= \Omega_0 + J\alpha + \Delta_\Omega \\ l &= (1+k)\alpha + \frac{2A}{a}[\sin(\alpha - \alpha_P) + \cos\alpha_P] \\ &\quad - 2c[1 - \cos((1+k)\alpha)] + \Delta_l \end{aligned}\right\} \qquad (2.6)$$

The secular variations caused by even zonals are described by the quantities ρ, J and k. ρ describes a constant shift in the mean orbital radius due to the extra terms in the potential. The secular change in the ascending node is described by J which gives a linear variation of Ω with time. The secular drift in the argument of latitude is described by k. The long periodic variations in the orbit are described by c and the short periodic variations are expressed as a Fourier series through the terms Δ_x for each of the four coordinates.

2.2 Update Epicycle Parameters

The changes in in-plane epicycle parameters due to a small delta-V can be found by differentiating the radial and azimuthal epicycle equations, and apply the assumption that the orbital velocity change is impulsive, so the position remains the same after firing:

$$\left.\begin{aligned} \hat{r} &= r \\ \hat{l} &= l \\ \hat{V}_r &= V_r + \Delta V_r \\ \hat{V}_q &= V_q + \Delta V_q \end{aligned}\right\} \qquad (2.7)$$

To first order, we can solve for the updated epicycle parameters as:

$$\left.\begin{aligned} \hat{a} &= a + \frac{2\Delta V_q}{n} \\ \hat{A} &= \sqrt{x^2 + h^2} \\ \hat{\alpha}_P &= \alpha - \tan^{-1}\frac{h}{x} \end{aligned}\right\} \qquad (2.8)$$

where:

$$\xi = A\cos(\alpha - \alpha_P) + \frac{2\Delta V_q}{n} + \frac{2\Delta V_q}{n} c\sin\beta$$

$$\eta = A\sin(\alpha - \alpha_P) + \frac{\Delta V_r}{n} - \frac{2\Delta V_q}{n} c\cos\beta$$

where $\beta = (1+k)\alpha$. Note that the change in A and α_P are functions of α whereas the change in a is not.

3. ORBIT DETERMINATION

UoSat-12 carries a GPS receiver, called SGR (Space GPS Receiver), developed by Surrey Satellite Technology Ltd. in collaboration with ESA. It is designed for micro or mini satellites and has 24 C/A code channels, weighs 1 kg and it only consumes 5.5 to 7 Watts power [11]. So that We have designed a Kalman filter based upon the epicycle description of orbit for UoSat-12 assuming GPS measurements are observable. We shall note we call GPS measurements for GPS receiver's position and velocity fix solutions. We have taken into account the secular perturbation effects to cover up to $O(10^{-6})$, which requires the modelling of J_2, J_2^2 and J_4 terms. The periodic variation need to be considered to $O(10^{-3})$ and which requires that J_2 short periodic, J_3/J_2 long periodic variations have to be included. The explicit coefficients related to this modelling are shown in [7].

We have addressed, however, in [5], it is preferable to model some extra terms to save the accuracy especially for UoSat-12 orbit, whose inclination angle is about 64.5° (note that the critical inclination is 63.4°). Because higher order long periodic terms J_{2m+1}/J_2 have $4-5\sin^2 I$ divisor, if the orbital inclination is near critical, then these terms may become comparable with (or larger than) J_3/J_2 term. Therefore the epicycle filter is designed to be able to optionally include J_5/J_2 and J_7/J_2 terms. Also some terms of tesseral/sectorial harmonic may cause sub-kilometre order m-daily variation in along-track direction. This is because some coefficients in tesseral/sectorial perturbation equation have ω_e/n divisor, where ω_e is the earth rotation rate and n is satellite mean motion, therefore typically which is $O(10^{-1})$. We show the peak along track variation due to $J_{lm} \equiv \sqrt{C_{lm}^2 + S^2{}_{lm}}$ tesseral/sectorial harmonic through J_{44} in *figure (3.1)*, where UoSat-12 orbit is assumed [12].

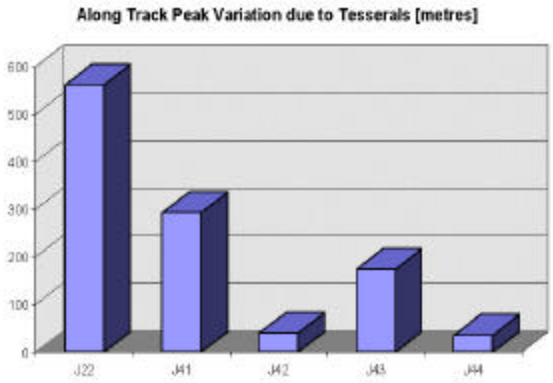

Figure 3.1 Peak Along Track Variation due to Tesserals

Because UoSat-12 orbital altitude is about 650 kilometres, the orbit perturbation caused by the atmospheric drag may not be negligible. In addition, we have solar maxima around year 2001. Therefore we incorporate a drag epicycle formulation assuming a constant atmospheric density, which shows the contribution of drag to semi-major axis and epicycle phase perturbations by:

$$\left.\begin{aligned} \hat{a} &= a - 2Ba \\ \hat{\alpha} &= \alpha + \frac{3}{2}Ba^2 \end{aligned}\right\} \qquad (3.1)$$

where *B* is some (drag) constant to be estimated by the filter. This basically says that the semi-major axis perturbation is linear to the time whereas the epicycle phase is quadratic.

The state parameter (or state vector) used is $\mathbf{x} = (a \;\; x_0 \;\; h_0 \;\; I_0 \;\; \Omega_0 \;\; \alpha_0 \;\; B)^T$ where x_0 and h_0 are given by:

$$\left.\begin{aligned} x_0 &= \frac{A}{a}\cos\alpha_P \\ h_0 &= \frac{A}{a}\sin\alpha_P \end{aligned}\right\} \qquad (3.2)$$

which enables us to avoid trying to determine A/a and α_P directly for these near circular orbits [13]. I_0 and Ω_0 are the osculating inclination and ascending

node at an initial ascending equator crossing and a_0 is the epicycle phase at the time when the first measurement is made. *B* is (optional) the drag parameter described in *equation (3.1)*. The measurements (or observation vector) are assumed to be $\mathbf{z} = (x \quad y \quad z)^T$ where x, y and z are the positional coordinates with respect to ECI (Earth Centred Inertial coordiante) directly converted from GPS position fix data from GPS receiver, which is with respect to WGS84 coordinate.

We have developed the recursive orbit estimator using the epicycle orbit description and we have used standard Kalman filter algorithm to design the estimator.

4. ORBIT CONTROL EXPERIMENT ON UoSat-12

We have conducted an experiment on precision repeat-groundtrack orbit insertion using low-thrust propulsion system on UoSat-12. A resonant condition which is a commensurability between the satellite's nodal frequency and the Earth's rotation rate can be formulated as:

$$kP_N(w_e - \dot{\Omega}) = 2pd \qquad (4.1)$$

where w_e is the Earth's rotation rate, $\dot{\Omega}$ is the drift rate in the longitude of the ascending node and P_N is nodal period of the orbit which is the period between successive equator crossings of the satellite, *d* is the integer number of days (nodal period of Greenwich) and *k* is the integer number of orbital revolutions of the repeating period. We have formulated this resonant condition in terms of the epicycle parameters as:

$$\frac{\left(\frac{w_e}{n} - J\right)}{(1+k)} = \frac{d}{k} \qquad (4.2)$$

Since n, J and k are functions of epicycle radius, a, and inclination, a resonant radius can be solved for, when the operational inclination given, by using a standard numerical method a resonant radius can be solved for by using a standard numerical method. *Equation (4.2)* allows us to use arbitrary numbers of terms in evaluating the resonant condition to any desired level of accuracy.

In our experiment, we aim to achieve a satellite groundtrack accuracy of less than *1 km* between consecutive cycles, and revisiting time error over any particular observation point to within *2 seconds*. This requires zonal harmonics up to J_4 to be included in the evaluation of resonant conditions. A resonant condition of 102 orbital revolutions in 7 days has been selected for UoSat-12. At the operational inclination of 64.57°, we can solve for a resonant radius of $a_0 = 7027.93 \pm 0.01$ km.

The spacecraft has been successfully placed into this resonant orbit on 7th December, 1999. The groundtrack is also phased so that the satellite passes directly over the ground station at SSC twice every week. *Figure (4.1)* shows the satellite groundtrack pattern around SSC after the orbit insertion (shown by thick lines). The pattern during the approach to resonance is also shown in the lighter lines.

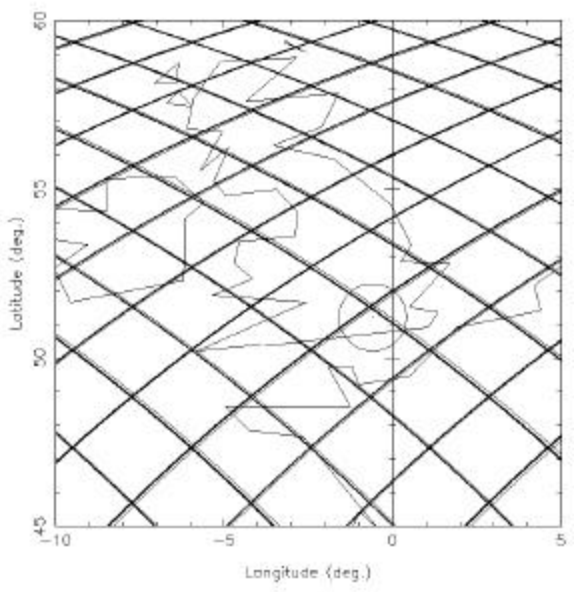

Figure 4.1 UoSAT-12 Groundtrack pattern around SSC before (light line) and after (thick line) the orbit insertion. The satellite passes directly over the ground station at SSC(marked by the centre of the circle) twice every week, and repeat every 102 orbital revolutions.

5. ORBIT MAINTENANCE

5.1 Resonant Orbit Maintenance

Atmospheric effects tend to cause the satellite orbit to decay secularly and causes the satellite groundtrack to drift eastward with respect to the reference track. To maintain the orbit at a resonant condition, we can set the drift rate to be positive at the beginning as we place the satellite just above resonance and allow drag to bring the orbit through resonance (see *figure (5.1)*). Because of drag, the drift rate will slow down and approaches zero, and the groundtrack drift reaches the maximum $\boldsymbol{s}$ when the semi-major axis is equal to the resonant value. The groundtrack starts to drift in the negative direction after that due to further drag, and must be compensated by a delta-V firing to maintain the satellite in resonance. Either the control frequency or the maximum drift in groundtrack can be specified in the evaluation of the required delta-V magnitude.

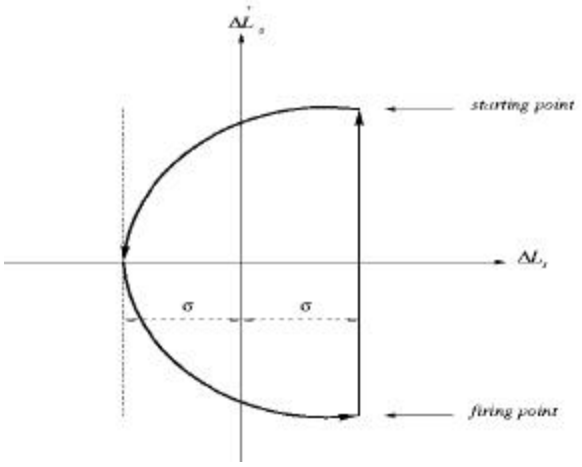

Figure 5.1 Phase plane diagram of the orbit maintenance strategy.

A small number of big burns strategy can reduce the frequency of orbit manoeuvres, but, on the other hand, a large number of small burns can maintain the satellite orbit using a small thrust propulsion system.

For the orbit maintenance of a small low-cost satellite, the small burn strategy is preferred. In fact, the long burn strategy will be more expensive on fuel. The upper and lower parts of the phase plane diagram shown in *figure (5.1)* will become more asymmetric when the period of a control cycle becomes longer because of the variation of the atmospheric density with height. This means that a bigger delta-V is required to restore the control loop.

An autonomous control system is ideal for maintaining the resonant orbit, because delta-V firing frequently can be performed frequently against drag effects. With real-time estimates of epicycle radius and decay rate onboard the satellite, a closed-loop controller can be designed to cope with the variations in atmospheric drag and maintain the control profile as described above. The impulsive control action is proportional to the deviation in semi-major axis from the resonant value and the orbital decay rate.

5.2 Maneouvring the orbit towards frozen condition

Under frozen conditions, the orbital eccentricity (e) and argument of perigee (w) are fixed in inertial space [8]. *Figure (5.2)* shows the evolution in e and w of UoSat-12 from the initial condition at epoch of simulation, and during 3 years of simulation period. It is obviously shown that the argument or perigee varies through 360° and the eccentricity variation exceeds 0.005. On the other hand, putting the satellite at the frozen condition conditions (in terms of epicycle parameters, e = 0.0035 and, $w = 270^\circ$ [9]) we will see small variations around a stable point (less than $\pm 30^\circ$ in w and 0.003 in e) as shown in *figure (5.3)*.

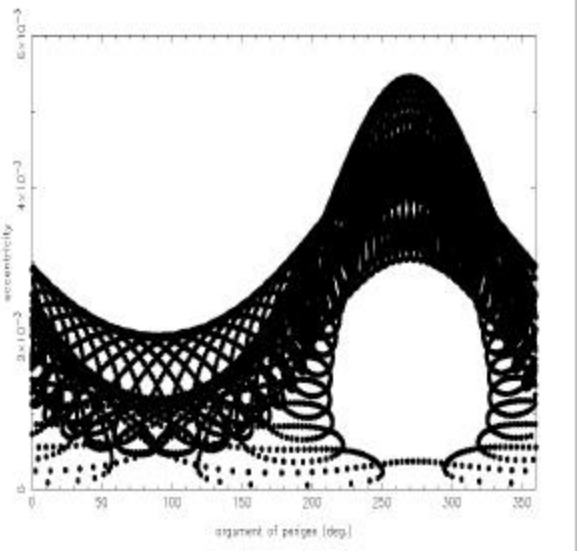

Figure 5.2 Evolution of eccentricity and argument of perigee of a non- frozen orbit.

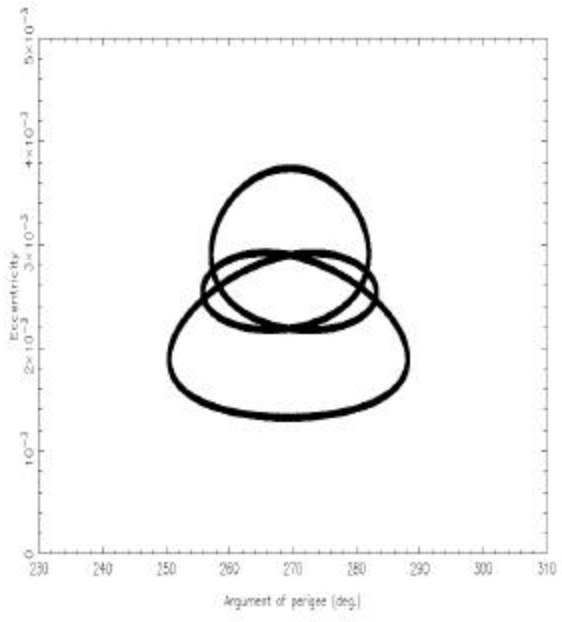

Figure 5.3 Small variations in eccentricity and argument of perigee around a frozen condition.

It has been shown that, to first order, the change in epicycle radius due to a small impulsive delta-V firing doesn't depend on the orbital phase at firing. We, therefore, have freedom in selecting the optimal firing phase for all small burns to shape the satellite orbit towards frozen conditions. The cost function, *J*, is simply introduced as the dot product between the target eccentricity vector and the actual change vector:

$$J = \Delta e_f . \Delta e_i + \Delta w_f . \Delta w_i \qquad (5.1)$$

where $(\Delta e_f, \Delta w_f)$ are the distance on the (e, w) plane from current state to frozen state, and $(\Delta e_i, \Delta w_i)$ are the actual change due to a small burn which are functions of orbital phase.

With a given delta-V vector, the steepest descent from an instantaneous (e, w) towards the target states can be found by maximising the cost function with respect to the orbital phase. The phase can then be directly converted to give the optimal firing time for each burn.

6. SYSTEM INTEGRATION

The control system comprises of the orbit determination system which estimates the epicycle as well as orbital decay rate parameters by using navigation data from the GPS receiver. The orbit controller calls for these parameters and calculates delta-V vector and optimal firing time. The controller feedbacks the predicted changes in parameters and covariance due to each delta-V to the determination system. The commands are sent to the manoeuver implementation system who validates the command within flight constraints and communicates with the attitude control system (ADCS) in order to turn the spacecraft accordingly to the commanded delta-V vector. Finally, if the command is valid, the propulsion system (the cold-gas thrusters in our case) is activated to execute the burn. Our control system can be summarised by the block diagram in *figure (6.1)*.

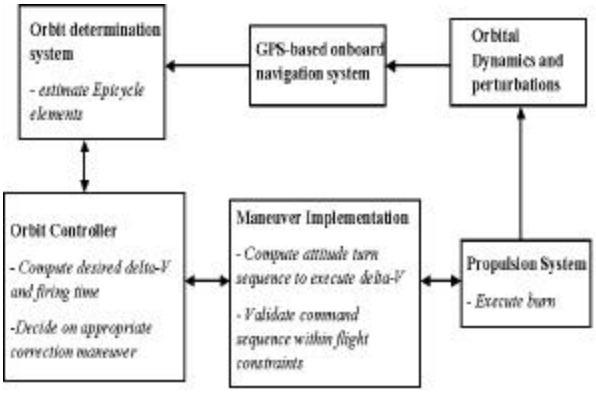

Figure 6.1 Autonomous Orbit Control System

The integration of control system has been preliminarily tested on an orbit control simulator developed at SSC. We have emulated GPS measurements by numerically integrating the satellite orbit using the high precision Bulirch Stoer integrator [10] with gausian noise added. Accuracy and speed of the integrator are very important in our long-term orbit maintenance simulation. The simulator also allows us to tune both the filter and controller parameters for the optimal values. The delta-V firings are emulated by impulsive change in velocity according to the controller commands while the remain the satellite's position. Again, gausian noise is merged to simulate the attitude and thrust level uncertainties.

7. EXPERIMENTAL RESULTS

During the 27 days of experimental period, the GPS receiver retrieves GPS navigation data every 10 seconds, and the orbit controller calls for determined epicycle elements every 24 hours to compute the firing commands. This control frequency was selected accordingly to the a priori decay estimation (about 10 m/day) and to average out the periodic effects from the tesseral and sectorial harmonics.

Figure (7.1) shows the estimated epicycle radius history (thick solid line) since this starting epoch until the end of the experiment 27 days later. The horizontal line in the graph is the reference epicycle radius, and the dotted lines around the estimated epicycle radius show the ± 5 metres ($3s$) error band according to determination accuracy .

The epicycle radius starts from approximately 30 m above the resonant value. The satellite could regulate the altitude at the resonant value without any support from the ground throughout the experiment. Most if the time, the epicycle radius remains within 5 m of the reference value with the RMS error of only *2.6* metres with respect to the estimated values. All delta-V commands are in the positive along-track direction which is the most effective use of the fuel. The delta-V magnitude history is shown in *figure (7.2)*. The mean delta-V during steady state is *3.6 mm/s*.

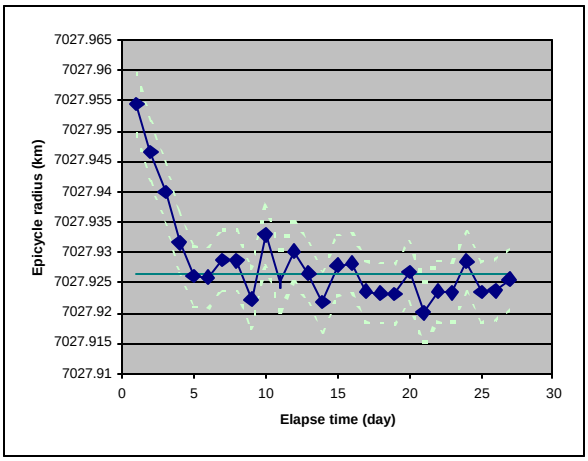

Figure 7.1 Epicycle radius history. The estimated epicycle radius is shown by thick solid line. The horizontal line is the reference value and the dotted lines around the estimated epicycle radius show the ± 5 metres error band according to determination accuracy.

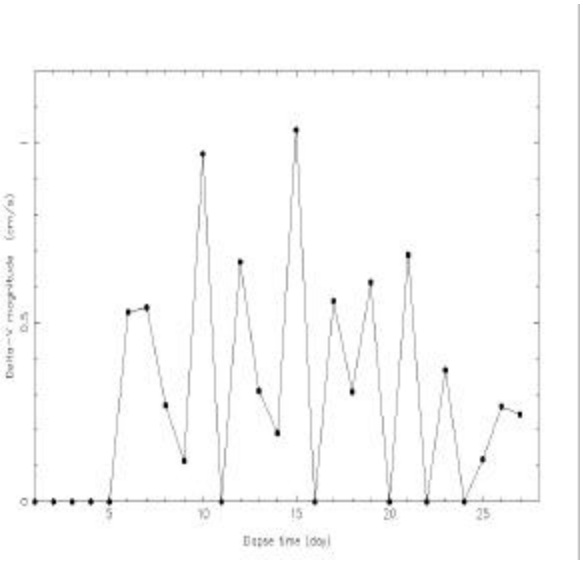

Figure 7.2 Delta-V magnitude history

8. CONCLUSIONS

We have successfully demonstrated an autonomous orbit maintenance system onboard a low-cost small satellite platform. Both orbit determination and control systems are designed and implemented through innovative epicycle parameters set. The demonstration was performed on maintaining an exact repeat-groundtrack orbit with an expected accuracy of better than 10 metres in mean radius around the resonant value. The results show that the spacecraft maintained itself in resonance within 3 metres ($1s$), with respect to the estimated values, around the commanded resonant altitude without any support from the ground. All tiny burns used for neglecting the daily drag effects are also optimally used for shaping the spacecraft orbit towards frozen conditions. This sophisticate integrated system have been achieved only by using low-cost in-house developed systems.

ACKNOWLEDGEMENT

The authors would like to take this opportunity to thank all supports from *SSC* ground operation and ADCS teams, and thank *Mahanakorn University*, Bangkok Thailand for their sponsorship for the conference.

REFERENCES

1. Chao C.C., Pollard J.E. and Janson S.W., "Dynamics and Control of Cluster Orbits for Distributed Space Missions", *AAS/AIAA Space Flight Mechanics Meeting*, Breckenride, Colorado, 7-10 Feb., 1999.

2. Busse, F.D., Inalhan, G. and How, J.P., "Project Orion: Precise Formation Flying Using Differential Carrier GPS", *AAS/AIAA Space Flight Mechanics Meeting*, Breckenride, Colorado, 7-10 Feb., 1999.

3. Bhat, R.S., Frauenholz R.B., and Cannell, P.E., "TOPEX/Poseidon Orbit Maintenance Maneuver Design", *Advance in the Astronautical Sciences*, Vol.71, Pt. 1, 1989, pp. 645-670.

4. Konigsmann H.J., Collins J.T., Dawson S. and Wertz, J.R., "Autonomous Orbit Maintenance System", *Acta Astronautica*, Vol.39, No.9-12, pp.977-985,1996.

5. Hashida, Y. and Palmer P.L., "Autonomous OnBoard Batch Filter for Near Circular Orbit Determination", *4th ESA International Conference on Spacecraft Guidance, Navigation and Control Systems*, ESTEC, Noordwijk, The Netherlands, 18-21 October 1999.

6. Fouquet M., Sweeting M., "UoSat-12 Minisatellite for High Performance Earth Observation at Low Cost", *47th International Astronautical Congress*, Beijing, 1996.

7. Hashida Y. and Palmer P.L., "Epicycle Motion of Satellites about an Oblate Earth", *Journal of Guidance, Control, and Dynamics.* , accepted for publication.

8. Cutting, E., Born, G.H., Frautnick, J.C., "Orbit Analysis For SEASAT-A", *The Journal of the Astronautical Science*, Vol. XXVI, No.4, pp.315-342, Oct.-Dec., 1978.

9. Aorpimai, A., Sreenuch T., Palmer, P.L., "A Strategy for UoSat-12 Frozen Orbit Insertion", *The Radio Amateur Satellite Organisation of The United Kingdom Conference*, 23-25 July, 1999, University of Surrey, Guildford, UK.

10. Palmer, P.L., Arseth, S.J., Mikkola, S., Hashida, Y., "High Precision Integration Methods for Orbit Propagation, *J. Astron. Sci*., 46, 329-342.

11. Unwin, M. J., Oldfield, M. K., "The Design and Operation of COT Space GPS Receiver.", *23rd Annual AAS Guidance and Control Conference*, Breckenridge, Colorado, USA, 2-6 February 2000.

12. Blizer, L. Astronautics 453, Handbookof orbital perturbations, University of Arizona

13. Cook, G. E., "Perturbations of near-circular orbits by the Earth's gravitational potential", *Planetary and Space Sci. , 14*, 433, 1966.